Thin Solid Films 551 (2014) 200–204

Contents lists available at ScienceDirect

Thin Solid Films

journal homepage: www.elsevier.com/locate/tsf

Strategies to control the spectral properties of Au–Ni thin films

David J. McPherson [a], Supitcha Supansomboon [a], Benjamin Zwan [b], Vicki J. Keast [b], David L. Cortie [c,d], Angus Gentle [a], Annette Dowd [a], Michael B. Cortie [a,*]

[a] Institute for Nanoscale Technology, University of Technology Sydney, PO Box 123, Broadway, NSW 2007, Australia
[b] School of Mathematical and Physical Sciences, University of Newcastle, Callaghan, NSW 2308, Australia
[c] Institute for Superconducting and Electronic Materials, University of Wollongong, Wollongong, NSW 2522, Australia
[d] Australian Nuclear Science and Technology Organisation, Lucas Heights, NSW 2234, Australia

ARTICLE INFO

Article history:
Received 3 August 2013
Received in revised form 28 November 2013
Accepted 29 November 2013
Available online 7 December 2013

Keywords:
Physical vapor deposition
Optical properties
Multilayers
Ab initio calculation
Gold–nickel

ABSTRACT

Gold and nickel have quite different dielectric functions. Here we use a combination of calculation and sample manufacture to assess two strategies by which thin films of these elements can be produced with a controlled range of far-field optical properties. In the first approach, control can be achieved by manipulating the density of states of metastable solid solutions, which in turn controls the dielectric function. In the second approach the optical properties of the films are controlled by varying the geometry of stacks fabricated from the constituent elements. We show that the two approaches can produce equivalent results so both are viable options in practice. Modeling is used to reveal how the structure controls the optical properties and to map out the possible color gamut. Predictions are tested with thin film samples fabricated by magnetron sputtering.

1. Introduction

The yellow color of bulk gold is the consequence of the element's unusual dielectric function [1]. Specifically, there is a well-defined band edge at about 2.4 eV (equivalent to green light, at a vacuum wavelength of about 515 nm). This band edge corresponds to the minimum photon energy capable of exciting electronic interband transitions from occupied to unoccupied states. Impinging photons of greater energy (i.e. shorter wavelength) are readily absorbed by the metal whereas photons of lesser energy will normally be scattered (reflected). Therefore, the reflectance of Au surfaces rises sharply as the wavelength of light is increased beyond the band edge. This results in the surface reflecting red, orange and yellow colors much more strongly than the blue to green colors, giving gold its characteristic color. In contrast, the band edge of Ag and most other metals lies in the UV, and hence they appear colorless (silver) to the human eye.

Here we analyze and compare two different microstructural strategies by which Ni can be used to modify the spectral properties of thin films of Au. The strategies are generic and, in principle, certain other elements, such as Fe, could be substituted for the Ni.

In the first approach we modify the electronic density-of-states (DOS) of the Au by adding Ni as an alloying element. This 'bleaches' (whitens) the color by modifying the location of the band edge and strength of the interband transitions [2–4]. Actually, while mutually soluble above 810 °C, the *equilibrium* solubility of Ni in Au, and vice versa, is negligible at room temperature because the binary phase diagram is characterized by a complete miscibility gap at room temperature [5], Fig. 1. Therefore, at first sight, bleaching of thin films of Au by modification of its band structure with Ni should not be possible at room temperature. Nevertheless, bleaching by this means is still feasible because metastable solutions of Ni in Au can be prepared, for example by annealing an alloy sample above 1000 K and then quenching it to room temperature, or by co-depositing Ni and Au onto a cold substrate using physical vapor deposition.

There have been only a few studies on the optical properties of such metastable Au–Ni alloys [6] or on those of the somewhat analogous Au–Fe system [7]. In general, the presence of transition metal impurities such as Ni is expected to generate a virtual bound state (VBS) within the conduction band of the Au [3,6] with the width of the VBS increasing as the impurity content increased [8]. This would cause enhanced scattering of conduction band electrons, i.e. a reduction in electrical conductivity, particularly at energies *below* the band edge [6]. This is usually correlated with an increase in optical 'loss' and decreased reflectance. However, the addition of Ni to Au concurrently causes a reduction of the interband absorption at energies *above* the band edge, in proportion to the quantity of Ni added [6]. The net result of these two opposing tendencies is that the reflectance at wavelengths above the band edge (i.e. towards the infrared) is reduced (due to the reduction in conductivity) while the reflectance at wavelengths below the band edge (i.e. towards the ultraviolet) is increased [3,6]. The overall effect is to de-saturate the color and, in the CIE $L^*a^*b^*$ color system, attenuate the luminance (brightness) of the alloy's surface.

---

[*] Corresponding author. Tel.: +61 2 9514 2208.
E-mail address: michael.cortie@uts.edu.au (M.B. Cortie).

0040-6090/$ – see front matter © 2013 Elsevier B.V. All rights reserved.
http://dx.doi.org/10.1016/j.tsf.2013.11.115

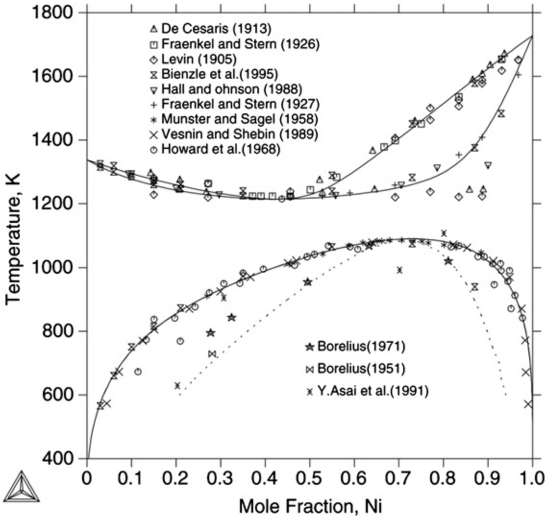

Fig. 1. Equilibrium phase diagram of the Au–Ni system. Reproduced with permission from J. H. Wang, X. G. Lu, B. Sundman, X. P. Su, *Calphad*, 2005, 29, 263 [14]. Copyright 2005, Elsevier. Note the negligible solubility of Au in Ni, or vice versa, at temperatures below about 400 K. The dotted line shows the estimated limit of the spinodal decomposition.

The second approach to controlling the spectral properties exploits the immiscibility of Au and Ni at room temperature. In this case the far-field spectral properties are derived from a nanoscale mixture of the pure elements. Provided the size scale of the nanostructure is well below the incident wavelength, light can penetrate through it and interact with buried features. The result is that the far-field optical properties of the alloy are a hybrid combination of those of the individual phases. In a sense, the heterogeneous microstructure may be thought of as a metamaterial whose effective dielectric properties are determined by the volume fraction and morphology of the Au and Ni regions and, possibly, by the amount of Ni remaining in the metastable solid solution of the Au-rich phase, and vice versa.

2. Methodology section

2.1. Calculations using density functional theory

In this study, calculations of the DOS for a number of different nickel concentrations were made using WIEN2k, an all-electron, linear augmented plane-wave density functional theory (DFT) code [9]. The complex dielectric function, $\varepsilon = \varepsilon_1 + i\varepsilon_2$, was calculated using the OPTIC routine within WIEN2k. These calculations are based on the random phase approximation and neglect local field effects [10]. The dielectric function was then used to obtain a theoretical reflectivity spectrum. The structures were generated by replacing atoms in the gold fcc structure with increasing numbers of Ni atoms. Note that WIEN2k does not simulate a random solid solution, and the Ni atoms in our simulations are on a periodic lattice. However, different configurations of Ni atoms were tested for $Au_{0.875}Ni_{0.125}$ and the effect on the optical response was found to be negligible. Similarly, relaxation of the lattice parameter of this alloy gave values to within 1% of that of pure Au and had a negligible effect on the optical response.

2.2. Optical property calculations

The properties of thin film stacks were modeled using OpenFilters [11]. This freely-available software calculates the optical properties of a stack of thin films using analytical expressions derived using the characteristic matrix approach. Colors are estimated by applying the CIE color space model, a standard illuminant (CIE-D65 white light) and a standardized observer (CIE-1964) to the calculated reflectance spectra. The published dielectric functions of bulk, annealed gold and nickel were used [12]. The simulations included 1 mm of fused SiO_2 glass as a substrate.

2.3. Preparation of thin films

The experimental samples for our study were deposited onto clear glass slides (Knittel Glaser). These had been cleaned by sonication in a sequence of acetone, ethanol and then water for 10 min at each step, rinsed with ultrapure water and immediately dried with N_2. Film fabrication was carried out using dual magnetron sputtering from Au and Ni targets of 50 mm diameter using independent control of electrical power (typically 62 W for the Au, with the power on the Ni target varied between 26 and 60 W). Deposition rates were calibrated using a quartz crystal sensor and were of the order of 0.1 to 0.3 $nm\cdot s^{-1}$ for the alloy. The substrate was at room temperature, the base pressure was about 1.3×10^{-4} Pa and the operating pressure in the chamber in the range 0.24 to 0.28 Pa for Ar. A rotating stage was used to provide a uniform coverage. In the case of multilayer samples, the first and last layers were Au, with the Au top layer intended to prevent oxidation of the Ni intermediate layer.

2.4. Characterization of thin films

Glancing angle X-ray diffraction (XRD) and X-ray reflectometry (XRR) was carried out on a PANanalytical X'Pert PRO diffractometer with a Cu-Kα source (0.15418 nm) in the standard Bragg–Brentano geometry. The accelerating voltage in both cases was 40 kV and the tube current 40 mA. The time per step was 5 s. For the XRD the step size was 0.05° and the angle of incidence (Ω) was 1°. For the XRR the step size was 0.005°. In both cases the beams were collimated and filtered.

Reflection and transmission spectra of the thin films were acquired using a Perkin Elmer 950 Lambda UV/Vis/NIR at an angle of incidence of 8° and a Varian Cary 5E UV/Vis/NIR at an incident angle of 0°, respectively. Estimates of the dielectric function of the alloy samples were extracted with WVASE32 (product of J A Woollam Co., Inc. of Lincoln, NE 68508, USA). The optical constants were obtained by fitting Lorentz oscillator models to the transmission and reflection spectra, which ensured the Kramers–Kronig consistency.

3. Results and discussion

3.1. Metastable (Au,Ni) alloys

Fig. 2 shows the total electronic DOS and the partial DOS for the Ni *d*-states for each alloy modeled. The DOS for pure gold is dominated by the *d*-band and the appearance of the transition metal dopant states (of Ni) as a VBS just below the Fermi level is clearly observed. The data are in qualitative agreement with the experimental valence band spectra for $Au_{(1-x)}Ni_x$ and with much earlier calculations [13].

The theoretical reflectivity spectra of Fig. 3a show that, as the nickel concentration increases, the reflectivity at long wavelengths should be attenuated relative to that of pure gold and the absorption edge should shift to shorter wavelengths (arrow). The calculated reflectivity of the $Au_{0.875}Ni_{0.125}$ compares very favorably to the measured reflectivity of a range of actual $Au_{0.85}Ni_{0.15}$ samples of different thickness, especially when referenced to pure Au, as shown in Fig. 3b. The changes in reflectivity can be attributed to the additional interband transitions from the VBS. At lower concentrations of Ni the theoretical reflectivity is intermediate in shape but the trend is not exactly monotonic indicating that precise details of the interband transitions are probably important. Once the alloy concentration increases to 25 at.% the Ni states appear to introduce an additional free-electron like contribution to the reflectivity and it evolves towards the reflectivity of pure Ni. At wavelengths shorter than the band edge, $Au_{0.875}Ni_{0.125}$ and $Au_{0.75}Ni_{0.25}$ have a reflectance greater than that of pure Au, i.e. their interband transitions have